FINITE ELEMENT MODELING OF A NONLINEAR POROMECHANIC DEFORMATION IN POROUS MEDIA

Manouchehr Sanei

manouchehr.sanei@gmail.com

Ph.D. Student in Petroleum Engineering

DEP-FEM-Universidade Estadual de Campinas, SP, Brazil

Omar Durán

omaryesiduran@gmail.com

Visiting Researcher

Center for Petroleum Studies CEPETRO - UNICAMP, SP, Brazil

Philippe R.B. Devloo

phil@fec.unicamp.br

Professor

FEC-Universidade Estadual de Campinas, SP, Brazil

Abstract. *Coupled fluid flow and deformation analysis in porous media is a remarkable subject in many engineering applications such as petroleum, civil, geothermal, biomechanical and nuclear engineering. Specifically, in petroleum applications the understanding of the poromechanic response of any petroleum reservoir is crucial for the accurate prediction of reservoir performance and evaluation of environmental impacts. Thus, this study develops an up to date coupled model between fluid flow and non-linear deformation in porous media, which delineates the complex multi-physics problem associated to reservoir depletion under solid deformation. The poromechanic analysis includes the linear component based on the Biot's theory and the nonlinear component based on the plastic deformation being established using the Drucker-Prager constitutive model. The fluid flow formulation in this coupling will be represented by the Darcy law. The numerical approximation lies on the Finite Element method with continuous Galerkin (CG) approximations for the* $\mathbf{u}$ / p *formulation, being* $\mathbf{u}$ *displacement and* p *pore pressure. Several simulations are compared with analytical and experimental data showing the validity of the computational implementation.*

Keywords: *Finite Elements, Poromechanic, Drucker-Prager, Porous Media*

1 INTRODUCTION

Porous media usually consist of a solid phase and pores filled up with one or more types of fluids. Some examples of porous materials are rocks, soils, concrete, and human bones, etc. Mechanical description of porous media, especially coupled flow deformation analysis is one of the most challenging subjects in many fields of engineering applications, including: reservoir engineering, enhanced oil recovery, petroleum drilling, nuclear waste storage, and geothermal energy among others (N. Khalili, Habte, and Zargarbashi, 2008).

In the last century, the petroleum industry has demanded a coupled model of fluid flow and non-linear deformation for applications in reservoir simulations that are devised to solve several engineering problems such as ground land subsidence, reservoir compaction, wellbore stability, and hydraulic fracturing. Originally, the coupled behavior of deformation and fluid flow was first developed under considerations of one-dimensional consolidation (Terzaghi, 1925). Subsequent to that pioneer research, the extension of the Terzaghi's theory to the third dimension was formulated by Biot, 1941. In numerical modeling (Chin, Raghavan, and Thomas, 2000) developed a two dimensional numerical approximation of a fully coupled fluid flow and rock deformation of wells with stress dependency. Several researchers emphasize that ignoring the coupling between fluid flow and rock deformation causes poor predictions for well damage, well placement, and reservoir performance (Minkoff, Stone, Bryant, Peszynska, and Wheeler, 2003). Furthermore, Dung, 2007 developed a fully coupled fluid flow and rock deformation model, to analyze the effect of reservoir compaction in porosity variations. Moreover, N. Khalili, Habte, and Zargarbashi, 2008 developed a fully coupled flow deformation model for cyclic analysis of unsaturated soils that included hydraulic and mechanical hysteresis. Recently, Wei and D. Zhang, 2010 developed a coupled fluid-flow and geomechanics for porosity/permeability changes in coalbed methane recovery. Also Ma, Zhao, and Nasser Khalili, 2016 developed a fully coupled flow deformation model for elastoplastic damage analysis in saturated fractured porous media.

Even though, significant advances have been published in porous media, the finding of a coupling between fluid flow and rock deformation is still not completely explored and understood. The aim of this research is to develop a coupling between fluid flow and non-linear deformation in porous media. This model consists of a linear component based on the Biot's theory and a nonlinear component based on plastic deformation using the Drucker-Prager constitutive model (Souza Neto, Peric, and Owen, 2008). The fluid flow formulation is based on Darcy's law and for coupling the conservation of mass and momentum are considered in a dimensionless form. The validity of the computational implementation is analyzed by comparing the results with analytical and experimental data.

2 GOVERNING EQUATIONS

The nonlinear poromechanical model includes of two components: the deformation and the flow model. The deformation model is established using an elastoplastic constitutive model and the flow counterpart is based on Darcy's law.

2.1 Momentum and mass conservation

The porous media is fully saturated with an incompressible fluid in a deformable porous medium. Ignoring the internal acting effects, the momentum conservation for the representative element of rock mass can be expressed as (Rudnicki, 1986):

$$\begin{aligned} \nabla \cdot \sigma_t + \mathbf{b} = 0 \\ and \\ \sigma_t = 2\,\mu\,\epsilon(\mathbf{u}) + \lambda tr(\epsilon(\mathbf{u}))I - \alpha\,p\,I \end{aligned} \tag{1}$$

In which $\mathbf{u}$ [m], σ_t [Pa], $\mathbf{b}$ [N m^{-3}], p [Pa], and α are displacement, total stress, body force, pore pressure, and Biot's poroelastic constant, respectively. The scalars λ [Pa] and μ [Pa] are the Lamé constants related to E [Pa] Young's modulus and υ Poisson ratio defined as:

$$\lambda = \frac{\upsilon E}{(1+\upsilon)(1-2\upsilon)} \tag{2}$$

$$\mu = \frac{E}{2(1+\upsilon)} \tag{3}$$

The corresponding initial (referred with the subscript $(\cdot)_\circ$) and boundary conditions as follows:

$$I.C. \;=\; \begin{cases} p_\circ = & p_\circ \\ \mathbf{u} = & \mathbf{u}_\circ \end{cases} \quad B.C. \;=\; \begin{cases} \sigma \cdot \mathbf{n} & on\ \partial\Gamma_{\sigma_t} \\ \mathbf{u} & on\ \partial\Gamma_u \end{cases} \tag{4}$$

As pointed out by (Rudnicki, 1986), the mass conservation is:

$$\tfrac{\partial}{\partial t}\left(\rho_f(\phi_\circ + \alpha\,(\nabla \cdot \mathbf{u} - \nabla \cdot \mathbf{u}_\circ) + S_\epsilon\,(p - p_\circ))\right) + \nabla \cdot \rho_f \bar{\mathbf{v}}_f \;\;=\;\; q_s \tag{5}$$

Where $\phi_\circ$ is the initial porosity, ρ_f [kg m^{-3}] is the fluid mass density, q_s [kg m^{-2} s^{-1}] is the sink flow , $S_\epsilon = \frac{1}{M}$ [Pa^{-1}] is the specific storage coefficient, and M [Pa] is the Biot's modulus (Herbert, 2002). In the case of incompressible fluids $S_\epsilon = 0$. The Darcy's law is written as:

$$\bar{\mathbf{v}}_f = -\tfrac{\kappa}{\eta}\,(\nabla p) \tag{6}$$

Where $\bar{\mathbf{v}}_f$ [m s^{-1}], η [Pa s], and κ [m^2] are the Darcy's velocity, fluid viscosity, and absolute permeability, respectively.

The corresponding initial and boundary conditions as follows:

$$I.C. = \begin{cases} p = \quad p_\circ \end{cases} \quad B.C. = \begin{cases} \bar{\mathbf{v}}_f \cdot n & on \ \partial\Gamma_q \\ p & on \ \partial\Gamma_p \end{cases} \tag{7}$$

2.2 Dimensionless expressions the poromechanic model

The momentum and mass conservation described in the last section for an incompressible fluid constituent are transformed by the dimensionless group presented in the Table 1.

Table 1: Group of dimensionless variables for an incompressible fluid.

$\mathbf{u}_D$	$\frac{\mathbf{u}}{Lp_0}\frac{(\lambda+2\mu)}{\alpha^2}$
λ_D	$\lambda\frac{\alpha^2}{(\lambda+2\mu)}$
μ_D	$\mu\frac{\alpha^2}{(\lambda+2\mu)}$
$\sigma_{t\ D}$	$\frac{\sigma_t}{p_0}$
$\mathbf{b}_D$	$\mathbf{b}\frac{L}{p_0}$
p_D	$\frac{p}{p_0}$
$\mathbf{q}_D$	$\mathbf{q}_f\frac{\eta}{\kappa}\frac{L}{\rho_f p_0}$
$\mathbf{v}_D$	$\mathbf{v}_f\frac{\eta}{\kappa}\frac{L}{p_0}$
x_D	$\frac{x}{L}$
t_D	$t\frac{c_f}{L^2}$

In Table 1, the quantities; p_0 [Pa], L [m], $\mathbf{q}_f$ [$m^3\,s^{-1}$], and c_f [$m^2\,s^{-1}$] are initial pore pressure, characteristic domain length, fluid rate, and hydraulic diffusivity, respectively.

The momentum conservation:

$$\nabla \cdot \sigma_{tD} + \mathbf{b}_D = 0 \tag{8}$$

$$\sigma_{tD} \quad = \quad 2\,\mu_D\,\epsilon(\mathbf{u_D}) + \lambda_D tr(\epsilon(\mathbf{u_D}))I \ \ - \alpha\, p_D\, I \tag{9}$$

The displacement boundary condition:

$$\mathbf{u}_D = \overline{\mathbf{u}}_D \quad on \quad \partial\Gamma_{u_D} \tag{10}$$

The total stress or traction boundary condition on $\partial\Gamma_{\sigma_t\,D}$:

$$\sigma_{t\,D} \cdot \mathbf{n} = \bar{\mathbf{t}}_D \quad on \quad \partial\Gamma_{\sigma_t\,D} \tag{11}$$

The mass conservation:

$$\nabla \cdot \mathbf{q}_D + \frac{\partial \phi^*_D}{\partial t_D} = 0 \tag{12}$$

The fluid mass content per unit of porous solid as follows:

$$\phi^* - \phi^*_\circ = (\alpha \nabla \cdot \mathbf{u}_D) \tag{13}$$

It is important to note that, the quantity ϕ^* is a nonlinear function by the sake of the nonlinearities presented in the deformation model. In this research the porosity is updated in an implicit way for every time step.

Darcy's law:

$$\mathbf{q}_D = -\nabla p_D \tag{14}$$

The pore pressure boundary condition:

$$p_D = \overline{p_D} \quad on \quad \partial\Gamma_{p_D} \tag{15}$$

The flux boundary condition:

$$-(\nabla \cdot p_D) \cdot \mathbf{n} = \bar{\mathbf{v}}_D \quad on \quad \partial\Gamma_{v_D} \tag{16}$$

3 ELASTO-PLASTIC CONSTITUTIVE MODEL

The elastoplastic formulation is represented by the theory of plasticity for the materials which present permanent deformations after some specific loading conditions. The plasticity mathematical framework can be described by dividing the total strain rate tensor into two parts, an elastic and plastic part. The elastic part is related to the current strain state and the plastic counterpart is related to the history of irreversible deformations that is mathematically described by three fundamental axioms: a yield criterion, a flow rule, and hardening law (Cecílio, Devloo, Gomes, Santos, and Shauer, 2015).

Yield criterion. Describes the transition between the elastic and plastic domains through a plasticity function ϕ [Pa]. The plasticity function assumes negative values in an elastic basis and null values in a plastic basis.

Flow rule. Assumes the existence of a plastic potential function ψ, which specifies how the plastic deformation tensor evolves in the plasticity process.

Hardening law. Specifies how the internal damage variable evolves.

In the present formulation, the yield surface and plastic potential are defined in the principal stress values space (Cecílio, Devloo, Gomes, Santos, and Shauer, 2015). The constitutive equation for the deformation of the solid skeleton is given by the following relationship between incremental elastic strain and incremental stress.

$$\dot{\sigma}_D = \mathbf{D}\dot{\epsilon} \tag{17}$$

Where $\mathbf{D}$ and $\dot{\epsilon}$ are the drained stiffness matrix and the incremental total strain rate of the soil skeleton, respectively.

Decomposition of strain tensor

The total strain rate $\dot{\epsilon}$ is obtained by splitting the tensor into the elastic component and a plastic component, as follows:

$$\dot{\epsilon} = \dot{\epsilon}^e + \dot{\epsilon}^p \tag{18}$$

Where, $\dot{\epsilon}^e$ elastic incremental strain and $\dot{\epsilon}^p$ plastic incremental strain are as follow:

$$\dot{\epsilon}^e = \nabla_{sym}\dot{\mathbf{u}}_{\mathbf{D}} \tag{19}$$

$$\dot{\epsilon}^p = \dot{\gamma}\mathbf{N} \tag{20}$$

Where $\dot{\gamma}$ and $\mathbf{N}$ are the plastic multiplier and plastic flow, respectively.

Plastic flow rule

In a loading cycle, when the stress state reaches a plastic regime, the material yields and the plastic strain evolutes according to the plastic flow rule. In this research is considered an associative plasticity model and the flow potential ψ is exactly to the yield function ϕ.

$$\psi = \phi \tag{21}$$

The plastic flow is:

$$\mathbf{N} = \frac{\partial \phi}{\partial \sigma_D} \tag{22}$$

3.1 Drucker-Prager Constitutive Model

This criterion was proposed as a smooth approximation to the Mohr-Coulomb law that consists of a modification of the von Mises criterion (Drucker and Prager, 1952). The plastic yielding begins when the J_2 invariant of the deviatoric stress and the hydrostatic stress $p_h\left(\sigma_D\right)$ reach a critical combination (Souza Neto, Peric, and Owen, 2008).

The hydrostatic stress is:

$$p_h\left(\sigma_D\right) = \frac{I_1}{3} \tag{23}$$

The yield function ϕ is as follows:

$$\phi(\sigma_D, c) = \sqrt{J_2(\mathbf{s}(\sigma_D))} + \eta p_h\left(\sigma_D\right) - \xi c \tag{24}$$

Where $c_D = \frac{c}{p_0}$ is the dimensionless cohesion and the parameters η and ξ are chosen according to the required approximation of the Mohr-Coulomb criterion.

The values of the parameters η and ξ at the compression cone:

$$\eta = \frac{6\sin\phi}{\sqrt{3}\left(3 - \sin\phi\right)} \tag{25}$$

$$\xi = \frac{6\cos\phi}{\sqrt{3}\left(3 - \sin\phi\right)} \tag{26}$$

The invariant of the deviatoric stress is:

$$J_2 = \frac{1}{2}\mathbf{s} : \mathbf{s} \tag{27}$$

Where $\mathbf{s}$ is the total deviatoric stress components:

$$\mathbf{s} = \sigma_D - p_h\, \sigma_D\, I \tag{28}$$

3.2 Integration algorithm for the Drucker-Prager

The algorithm of return-mapping has been implemented using the Newton method on the cone and the apex of the model. The flow vector for Drucker-Prager is given by:

$$\mathbf{N} = \frac{\partial\phi}{\partial\sigma_D} = \frac{1}{2\sqrt{J_2(s)}}s + \frac{\eta}{3}I \tag{29}$$

The corresponding increment of plastic strain in the cone reads:

$$\Delta\ \dot{\epsilon}^p = \Delta\gamma\ \mathbf{N} \tag{30}$$

A simplified return-mapping update formula without hardening for the stress tensor for materials with elastic law is:

$$\sigma_{D\ n+1} = \sigma_{D\ n+1}^{trial} - \Delta\gamma D^e : \mathbf{N}_{n+1} \tag{31}$$

Where $-\Delta\gamma D^e : \mathbf{N}_{n+1}$ is the return vector.

The consistency condition of the cone for $\Delta\gamma$ is as follows:

$$\tilde{\phi}(\Delta\gamma) = \sqrt{J_2(s_{n+1}^{trial})} - \mu_D\Delta\gamma + \eta - \xi c_D = 0 \tag{32}$$

The nonlinear process is to solve for $\Delta\gamma$ such that the consistency condition $\tilde{\phi} \approx 0$, following the group of Eq. (29), (30), (31), and update the elastoplastic variables. This process is repeated overall integration points in the following finite element scheme.

4 Variational Formulation

This section establishes the weak form of the strong formulation of the nonlinear poromechanic problem described above.

Weak form

By following the standard arguments of variational principles, the function spaces to approximate the state variables $\mathbf{u}_D$ and p_D, that are defined as follows:

V : function space of displacement field $\mathbf{u}_D$, defined by:

$$V = \left\{ f \in H^1(\Omega),\ f = u_D\ on\ \partial\Omega_1 \right\} \tag{33}$$

W : function space of pore pressure field p_D, defined by:

$$W = \left\{ f \in H^1(\Omega),\ f = p_D\ on\ \partial\Omega_2 \right\} \tag{34}$$

Where H^1 is the Hilbert space of order one. For the definition of the continuous Galerkin approximation, it is required the discretization of the temporal and spatial domains. The representation of the discrete state variables ($\mathbf{u}_h$ and p_h, here for simplicity the dimensionless subscript D is dropped out) as linear combinations of finite dimensional subspaces V_h of Eq. (33) and W_h of Eq. (34), it is the principle that allows to obtain a systematic way to construct a linear system of equations, that comes from the linearization of the nonlinear poromechanic problem. The discrete weak statement of the nonlinear poromechanic deformation with initial and boundary conditions is described in the next subsections.

Weak form of mass conservation

By multiplying the mass conservation equation by $w_h \in W_H$ and integrating over the spatial domain, the following equation is obtained:

$$\int_{\Omega} \left(\frac{\Delta\phi^*}{\Delta t}\right) w_h \, \partial\Omega + \int_{\Omega} (\nabla p_h) \cdot \nabla w_h + \int_{\Gamma_{Neumman}} w_h q_{D\,normal} \, \partial\Gamma = 0 \tag{35}$$

Note that the above form only involves first derivatives of quantities instead of the second derivatives in the original differential equation:

Weak form of momentum conservation

By multiplying the momentum conservation equation by $\mathbf{v}_h \in V_h$ and integrating over the spatial domain, the following equation is obtained:

$$\int_{\Omega} (\nabla \cdot \sigma_{tD} + \mathbf{b}_D) \cdot \mathbf{v}_h \, d\Omega = 0 \tag{36}$$

Inserting the linear poroelastoplastic constitutive equation

$$\begin{aligned} -\int_{\Omega} \left(\lambda_D \left(\epsilon_{vh}\left(\mathbf{u}_h\right)\right) + 2\mu_D \epsilon\left(\mathbf{u}_h\right)\right) \cdot \epsilon\left(\mathbf{v}_h\right) \, d\Omega + \int_{\Omega} \left(\alpha\left(p_h\right) I \cdot \nabla \mathbf{v}_h\right) \, d\Omega \\ + \int_{\Gamma_{Neumman}} \left(\sigma_{tD} \cdot \mathbf{n}\right) \cdot \mathbf{v}_h \, \partial\Gamma + \int_{\Omega} \mathbf{b}_D \cdot \mathbf{v}_h \, d\Omega = 0 \end{aligned} \tag{37}$$

In this research instead to construct the global tangent operator, we select the secant method to solve the nonlinear system. The approximation of the tangent matrix is just the linear operator corresponding to the linear poroelasticity Biot's operator.

5 RESULTS AND DISCUSSIONS

Numerical implementation of the nonlinear poromechanic deformation in porous media is accomplished through the finite element approach briefly detailed above. The governing equations are discretized spatially using the standard Galerkin method. It is well known, that in finite element spaces for poroelasticity, the approximation spaces must satisfy some compatibility conditions, in order to fulfill the stability criteria dictated by Babuska-Brezzi condition, the displacement approximation order should be one order greater than the pore pressure approximation order (Murad and Loula, 1992). In order to verify the numerical approximation the following analytical solution is used and compared with the proposed numerical implementation.

5.1 Finite poroelastic column

In Terzaghi's classical consolidation test the poroelastic column is finite i.e. a half-space. A constant stress is applied suddenly on the surface $y = 0$ of a fluid saturated column of length L [m]. This problem is analogue to an early time solution for a semi-infinite column with the same boundary condition and step load. Dimensionless forms of these equations are given by Korsawe, Starke, Wang, and Kolditz, 2006 as:

Pore pressure:

$$p_D\left(y_D, t_D\right) = \sum_{n=0}^{\infty}\left(\frac{2}{M} sin\left(M \cdot x_D\right) \exp^{-M^2 t_D}\right) \tag{38}$$

Displacement:

$$\mathbf{u}_{yD}\left(y_D, t_D\right) = 1 - x_D - \sum_{n=0}^{\infty}\left(\frac{2}{M} cos\left(M \cdot x_D\right) \exp^{-M^2 t_D}\right) \tag{39}$$

Darcy velocity:

$$\mathbf{v}_D\left(y_D, t_D\right) = -\sum_{n=0}^{\infty}\left(2cos\left(M \cdot x_D\right) \exp^{-M^2 t_D}\right) \tag{40}$$

Where $M = \frac{1}{2}\pi\left(2n + 1\right)$. These expressions are compatible with the variables defined in Table 2:

α	λ_D	μ_D	σ_{tD}	Δt_D
1.0	0.25	0.375	1.0	1.0×10^{-5}

Table 2: Dimensionless data used in the numerical verification.

An excellent fit is obtained for the state variables shown in figures 1 and 2.

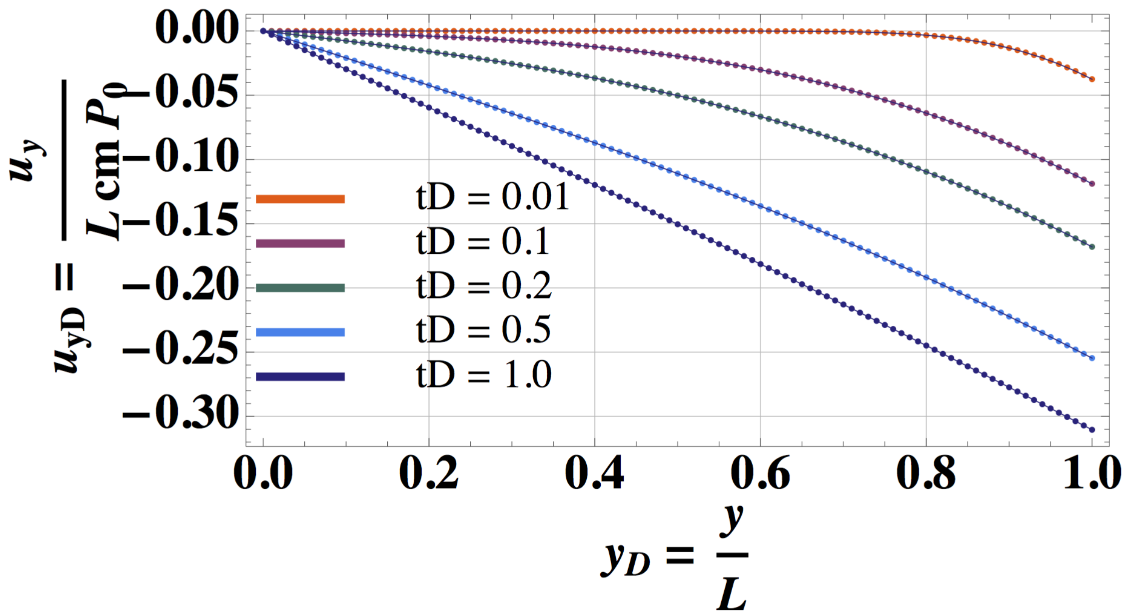

Figure 1: Dimensionless displacement at several dimensionless times.

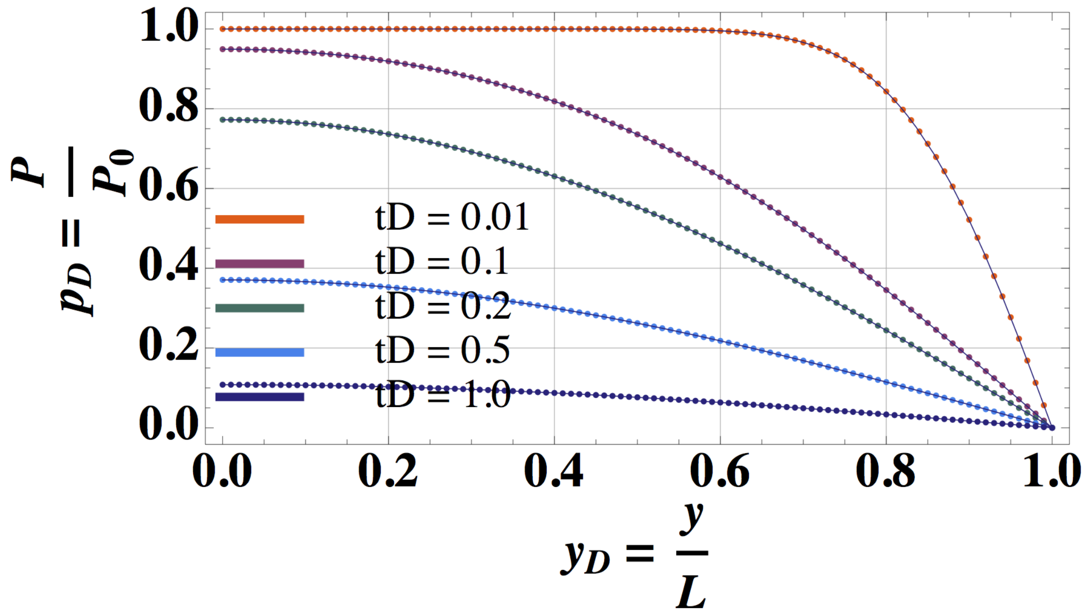

Figure 2: Dimensionless pressure at several dimensionless times.

5.2 Numerical Model Validation

As reported by (C.-L. Zhang, 2016) the triaxial compression test was carried out on the samples that were extracted from the Callovo-Oxfordian argillaceous formation to analyze the stress strain permeability behavior of clay rock. The average physical properties of the samples are: density 2700 $[\mathrm{kg\,m^{-3}}]$, porosity 0.168, and water saturation 0.96 (almost full saturated sample) and the size of core samples is 70 $[\mathrm{m^{-3}}]$ diameter and 140 $[\mathrm{m^{-3}}]$ length. The samples were sequentially loaded to analyze the stress-strain behavior of rock with permeability dependency.

To evaluate the accuracy of the nonlinear poromechanic deformation model, the triaxial compression test proposed by Zhang (2016) is approximated by our finite element implementation. The input and material parameters for finite element analysis are the same as the real test data. The validity of the model is investigated by comparing numerical results with experimental test data in three types, including: a) radial strain versus differential stress, b) volumetric strain versus differential stress, and c) axial strain versus differential stress. From Fig. 3, it can be seen that the numerical results are in good agreement with the experimental test data.

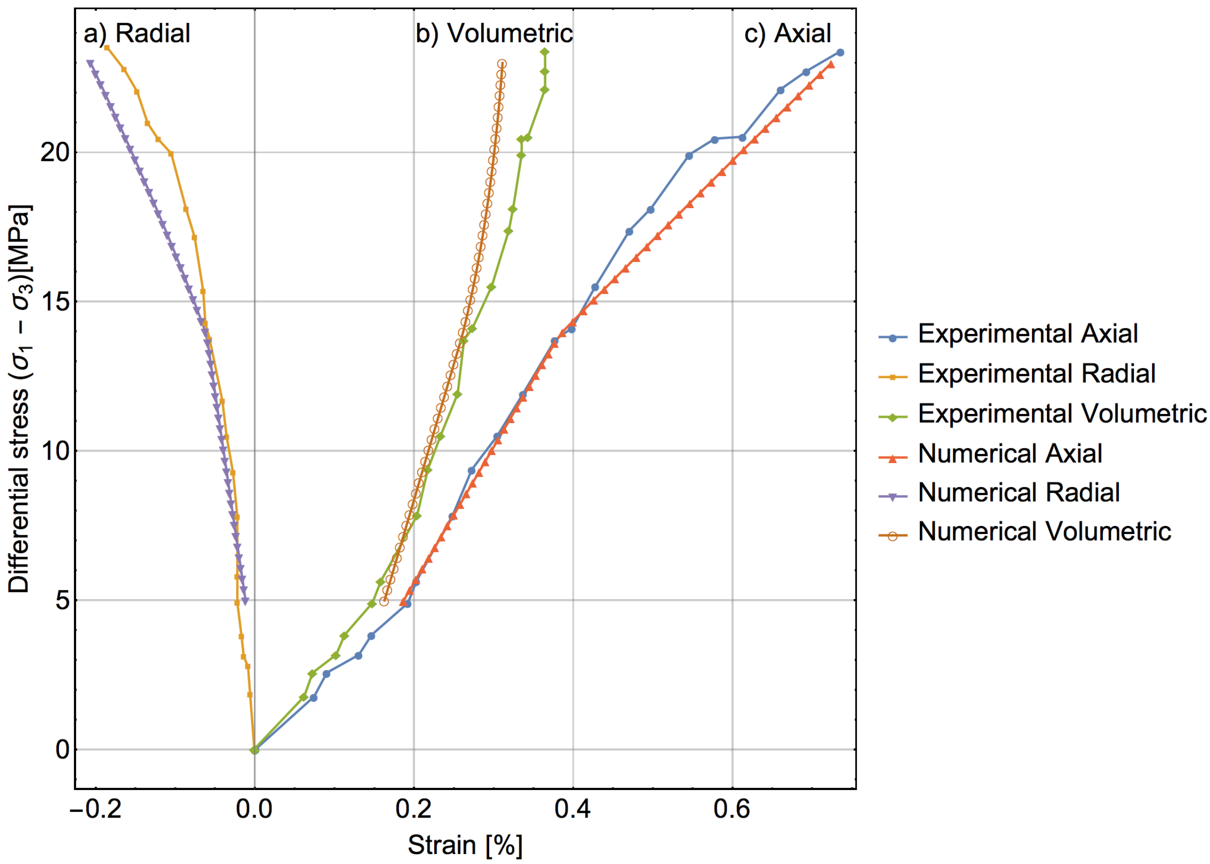

Figure 3: Validation of the model by comparing the numerical approximation of the triaxial compression test.

5.3 The nonlinear effect of plastic deformation

In order to show the nonlinear effects, a poroelastoplastic consolidation is approximated and compared with the linear poroelastic response in terms of porosity variation. The physical setting is similar to the poroelastic consolidation presented before in the section 5.1 with additional modifications. The column has an initial porosity ϕ_0 and it is precompacted with a predefined stress σ_0 [MPa], then a time dependent load is applied on the top of the column $\sigma_{top} = 25 \times t$ [MPa]. The final time is $t = 0.0001$ [s], and the poroelastoplastic parameters are given in the Table 3.

Table 3: Poroelastoplastic parameters used for the nonlinear consolidation.

λ [Pa]	μ [Pa]	ϕ_0	α	c [MPa]	ϕ [°]	Δt [s]	L [m]	d [m]
1211.5×10^6	1817.25×10^6	0.168	0.7	21	21	1.0×10^{-6}	0.140	0.07

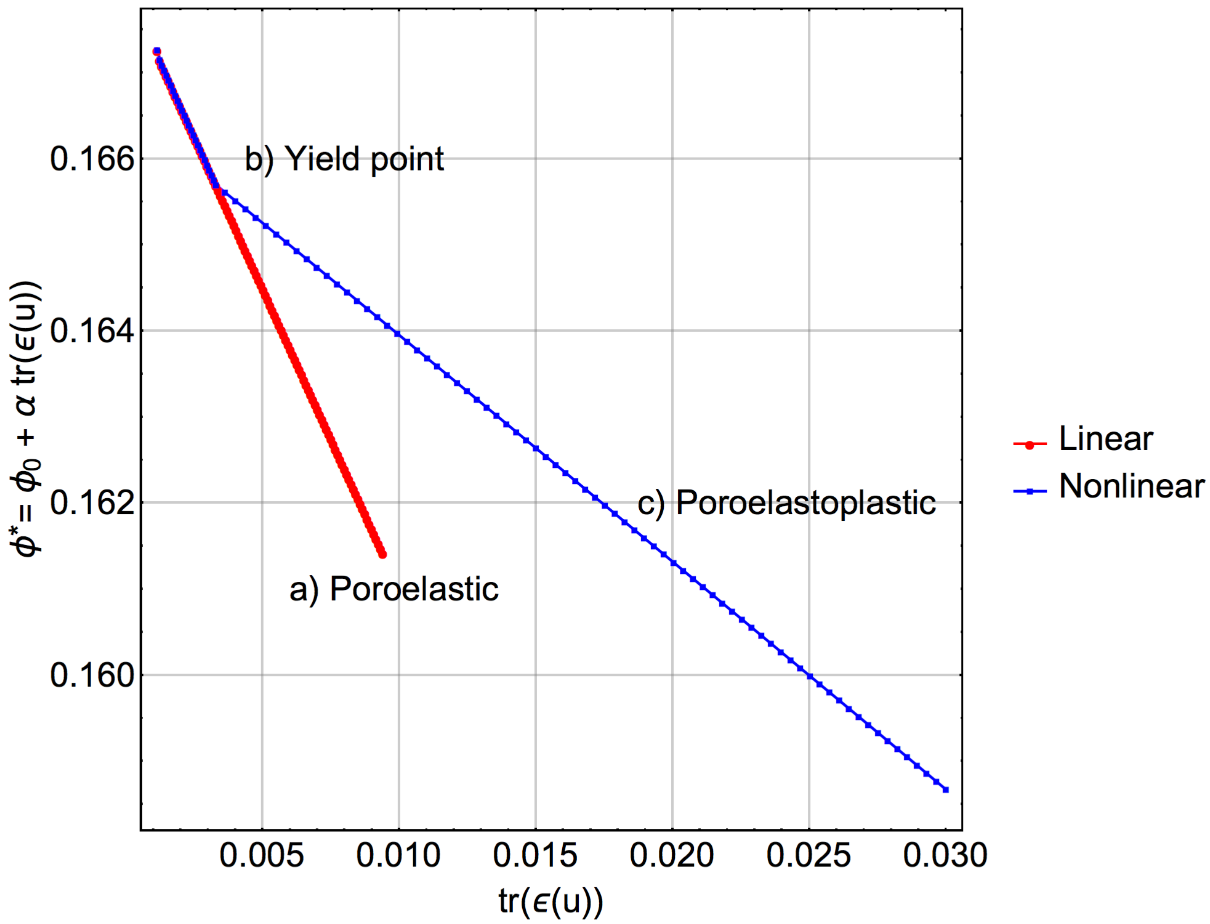

Figure 4: Volumetric strains versus porosity variation.

The effect of the nonlinear poromechanic is presented in Fig.4. By isolating the fluid compressibility effect (see Eq. (13)), it can be shown that the porosity variation is also a linear function of the volumetric strain. It can be observed from the yield point (see Fig.4 b)) that the elastic prediction (see Fig.4 a)) underestimates the change of porosity, when it is compared with the nonlinear deformation (see Fig.4 c). That suggests us the necessity for the nonlinear behavior, and it is important to remark that this effect is more evident in unconsolidated rocks.

6 CONCLUSIONS

Based on the importance of the coupling between fluid flow and deformation in petroleum engineering, a nonlinear poromechanic deformation model is proposed for porous media. This model develops an up to date coupled model between fluid flow and non-linear deformation. Two main components of the model are identified: the deformation and flow. The poromechanic analysis includes the linear component based on the Biot's theory and the nonlinear component based on the plastic deformation using the Drucker-Prager constitutive model. The fluid flow formulation in this coupling is represented by the Darcy's law. The numerical approximation is done by the Finite Element method with stable continuous Galerkin approximations for the $\mathbf{u}$ / p formulation. Good agreement between numerical simulation with both, analytical and experimental data evidences the capability of the proposed computational model to approximate the coupling between fluid flow and deformation in porous media.

In order to demonstrate the nonlinear poromechanic deformation a comparison with the linear poromechanic response is presented in the framework for the column consolidation. The comparison shows even for incompressible fluids, the effect of the nonlinear deformation, on porosity variation is observed by comparing it with the linear response, which underestimates the porosity changes, and suggests the need for the nonlinear models.

ACKNOWLEDGEMENTS

The authors M. Sanei, O. Durán and P.R.B. Devloo thankfully acknowledge financial support from the Brazilian National Agency of Petroleum, Natural Gas and Biofuels (ANP-PETROBRAS).

REFERENCES

Biot, Maurice A. (1941). "General Theory of Three-Dimensional Consolidation". In: *Journal of Applied Physics* 12.2, pp. 155–164.

Cecílio, Diogo L., Philippe R.B. Devloo, Sônia M. Gomes, Erick R.S. dos Santos, and Nathan Shauer (2015). "An improved numerical integration algorithm for elastoplastic constitutive equations". In: *Computers and Geotechnics* 64, pp. 1–9.

Chin, L.Y., R. Raghavan, and L.K. Thomas (2000). "Fully Coupled Analysis of Well Responses in Stress-Sensitive Reservoirs". In: *SPE Reservoir Evaluation & Engineering* 3.05, pp. 435–443.

Drucker, D. C. and W. Prager (1952). "Soil mechanics and plastic analysis or limit design". In: *Quarterly of Applied Mathematics* 10.2, pp. 157–165.

Dung, T.Q. (2007). "Coupled fluid flow-geomechanics simulations applied to compaction and subsidence estimation in stress sensitive & heterogeneous reservoirs". PhD thesis. PhD thesis. University of Adelaide: Department of Australian School of Petroleum.

Herbert, F. Wang (2002). *Theory of Linear Poroelasticity-with Applications to Geomechanics and Hydrogeology.* Vol. 150. 3. Oxford University Press (OUP), pp. 828–829.

Khalili, N., M.A. Habte, and S. Zargarbashi (2008). “A fully coupled flow deformation model for cyclic analysis of unsaturated soils including hydraulic and mechanical hystereses”. In: *Computers and Geotechnics* 35.6, pp. 872–889.

Korsawe, Johannes, Gerhard Starke, Wenqing Wang, and Olaf Kolditz (2006). “Finite element analysis of poro-elastic consolidation in porous media: Standard and mixed approaches”. In: *Computer Methods in Applied Mechanics and Engineering* 195.9-12, pp. 1096–1115.

Ma, Jianjun, Gaofeng Zhao, and Nasser Khalili (2016). “A fully coupled flow deformation model for elasto-plastic damage analysis in saturated fractured porous media”. In: *International Journal of Plasticity* 76, pp. 29–50.

Minkoff, Susan E., C. Mike Stone, Steve Bryant, Malgorzata Peszynska, and Mary F. Wheeler (2003). “Coupled fluid flow and geomechanical deformation modeling”. In: *Journal of Petroleum Science and Engineering*, pp. 37–56.

Murad, Márcio A. and Abimael F.D. Loula (1992). “Improved accuracy in finite element analysis of Biot’s consolidation problem”. In: *Computer Methods in Applied Mechanics and Engineering* 95.3, pp. 359–382.

Rudnicki, John W. (1986). “Fluid mass sources and point forces in linear elastic diffusive solids”. In: *Mechanics of Materials* 5.4, pp. 383–393.

Souza Neto, E. A. de, D. Peric, and D. R. J. Owen (2008). *Computational Methods for Plasticity: Theory and Applications*. Wiley.

Terzaghi, Karl (1925). “Erdbaumechanik auf bodenphysikalischer grundlage, Franz Deutikle, Leipzig und Wien”. In:

Wei, Zhijie and Dongxiao Zhang (2010). “Coupled fluid-flow and geomechanics for triple-porosity/dual-permeability modeling of coalbed methane recovery”. In: *International Journal of Rock Mechanics and Mining Sciences* 47.8, pp. 1242–1253.

Zhang, Chun-Liang (2016). “The stress–strain–permeability behaviour of clay rock during damage and recompaction”. In: *Journal of Rock Mechanics and Geotechnical Engineering* 8.1, pp. 16–26.